

Approximating the Medial Axis by Shooting Rays: 3D Case

Svetlana Stolpner*

Kaleem Siddiqi†

Sue Whitesides‡

Abstract

We consider an algorithm, first presented in [13], that outputs regions intersected by the medial axis of a 3D solid. In practice, this algorithm is used to approximate the medial axis with a collection of points having a desired density. The quality of the medial axis approximation is supported by experimental results. Despite promising 2D results, the algorithm’s theoretical guarantees are not understood in 3D. The contribution of this article is to initiate the 3D theoretical analysis by presenting properties of medial points that are not detected by the algorithm for a finite sampling rate.

1 Introduction

Consider an orientable 3D solid Ω with boundary \mathcal{B} .

Definition 1 *The medial axis \mathcal{MA} of Ω is the set of centres of maximal (for the inclusion order) inscribed balls in Ω .*

For example, Figure 1 shows the medial axis of a box. Figure 3 shows subsets of medial axes of more complex inputs. The medial axis, introduced in [3], is a valuable shape descriptor with applications to computer vision, computer graphics, GIS and robotics [11], as it captures local width information and part structure. Computing an accurate, robust, and useful shape descriptor based on the medial axis for complex 3D inputs remains a subject of ongoing research. In this article, we study the theoretical properties of an algorithm for medial axis approximation, which is shown to be successful at generating qualitatively meaningful approximations in practice in [14]. The following definition will be central:

Definition 2 *The Euclidean distance transform of Ω is given by $D(p) = -\inf_{q \in \mathcal{B}} d(p, q)$, where $p \in \Omega$ and $d(p, q)$ denotes Euclidean distance.*

The gradient of D , $\nabla D : \mathbb{R}^3 \rightarrow \mathbb{R}^3$ is a vector field that assigns each point p the direction to its nearest point on \mathcal{B} , whenever this direction is uniquely defined.

The vector field ∇D is uniquely defined for all points inside Ω except for those on the medial axis. As medial points have two or more nearest boundary locations, ∇D is multi-valued on the medial axis. This property is the basis for Algorithms 1 and 2 that locate medial points: we will look for regions where ∇D is multi-valued.

Given a medial point $m \in \mathcal{MA}$, equidistant from exactly two boundary points, the directions to its nearest boundary points are called the *spoke vectors*. The angle between the two spoke vectors is twice the *object angle* of m . The object angle θ in Figure 1 is $\pi/4$. The distance from m to \mathcal{B} is the *radius* of m . Object angle and radius are popular measures used to guide pruning of “insignificant” medial points [6, 8, 2, 12].

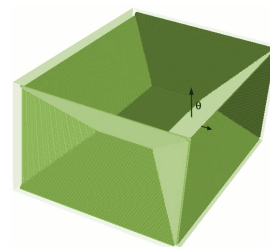


Figure 1: The medial axis of a box.

Previous Work When Ω is a polyhedron, [5] computes the edges of the medial axis of a polyhedron with a small number of faces using exact arithmetic. For objects whose boundary is given as a set of points, [1, 6] approximate the medial axis using a subset of the Voronoi vertices of the set of boundary points, and show convergence for a sufficient sampling density. However, these methods are very sensitive to noise in the boundary samples, and numerous techniques have been proposed to prune undesirable portions of the computed medial axes [15, 9]. Methods [7, 16, 4] recursively subdivide space and consider the nearest boundary elements to the spatial regions. Accuracy is guaranteed when approximating the generalized Voronoi diagram, where the diagram is localized by for a sufficiently small spatial resolution. The average outward flux of ∇D in a region shrinking to zero is used to decide the presence of medial points in [10]; this concept is generalized to non-zero regions for polyhedral inputs in [12]. Several methods consider angles between ∇D vectors for pairs of points p, q and conclude that a medial point exists on the midpoint of (p, q) if the two vectors’ tails are closer than their tips [17, 8].

Organization and Main Results Section 2 reviews algorithms that analyze ∇D vectors for points sampled

*School of Computer Science and Centre for Intelligent Machines, McGill University, sveta@cim.mcgill.ca

†School of Computer Science and Centre for Intelligent Machines, McGill University, siddiqi@cim.mcgill.ca

‡Department of Computer Science, University of Victoria, sue@uvic.ca.

on the boundary of a sphere to determine if the sphere contains a medial point, and if so, its approximate location. We include experimental results that show collections of medial points computed using this method, where the density of medial points is user-prescribed. Our main results are found in Section 3, which discusses the positions of points to be sampled on the sphere, and Section 4, which establishes the locations of nearest boundary points to medial points that are not detected by our algorithm for a finite sampling rate. Section 5 presents avenues for future work.

2 Shooting Rays Algorithm

Our algorithm for medial axis approximation is based on the following property of ∇D :

Lemma 1 ([13]) *Let p be a point in Ω that is not a medial point. Let $q = p + \gamma \cdot \nabla D(p)$, such that γ is a scalar, q is not a medial point, and (p, q) lies inside Ω . A medial point of Ω lies on (p, q) if and only if $\nabla D(p) \neq \nabla D(q)$.*

Consider a point p on a sphere S . Let l be a line through p with direction $\nabla D(p)$. Define the *opposite* of p , $opp(p)$, to be the other point of intersection of l with the surface of S . In case $\nabla D(p)$ is tangent to S at p , $opp(p) = p$. Algorithm 1 uses a technique we call *shooting rays* to conclude that a sphere is intersected by the medial axis, when evidence of this is found. If a medial point lies in S , Algorithm 1 will necessarily return ‘True’ for a sufficiently dense set of points Φ . However, for a finite Φ , a medial point may lie in S , while Algorithm 1 returns ‘Undecided’.

Algorithm 1 DECIDEMA(\mathcal{B}, S, Φ)

Require: Boundary \mathcal{B} , sphere S , not intersecting \mathcal{B} , set of points Φ distributed on S .

Ensure: ‘True’ if S contains a medial point, ‘Undetermined’ if no such conclusion can be drawn.

```

1: for all  $\phi_i \in \Phi$  do
2:   if  $\phi_i$  or  $opp(\phi_i)$  is a medial point then
3:     Return ‘True’
4:   end if
5:   if  $\nabla D(\phi_i) \neq \nabla D(opp(\phi_i))$  then
6:     Return ‘True’
7:   end if
8: end for
9: Return ‘Undetermined’

```

Algorithm 2 performs binary search to estimate the intersection of the medial axis with a line segment to a desired accuracy ϵ . As discussed in [14], we have successfully used Algorithm 2 to detect medial points for polyhedral inputs. In our implementation, the interior of a polyhedron is partitioned into regular sized

Algorithm 2 RETRACT($p, q, \mathcal{B}, \epsilon$)

Require: Non-medial points p, q interior to \mathcal{B} s.t. $q = p + \gamma \cdot \nabla D(p)$ and $\nabla D(p) \neq \nabla D(q)$, tolerance ϵ .

Ensure: A point within ϵ of the medial axis of \mathcal{B} .

```

1: while  $d(p, q) > \epsilon$  do
2:    $m = \frac{1}{2}(p + q)$ 
3:   if  $m$  is a medial point then
4:     Return  $m$ .
5:   end if
6:   if  $\nabla D(m) \neq \nabla D(p)$  then
7:      $q = m$ 
8:   else
9:      $p = m$ 
10:  end if
11: end while
12: Return  $p$ .

```

cubes (voxels) and a sphere is circumscribed about each voxel. For those spheres deemed intersected by the medial axis, we compute the approximate locations of a medial point inside this sphere using Algorithm 2. Among the approximate medial points found in a sphere circumscribed about voxel v , we store a single point that lies inside v and has a sufficiently high object angle. The voxel size determines the density of the computed set of medial points. Figure 3 presents examples of the medial points computed by our method for several polyhedra of significant geometric complexity. Figure 2 shows the effect of varying the voxel size on the density of medial points computed.

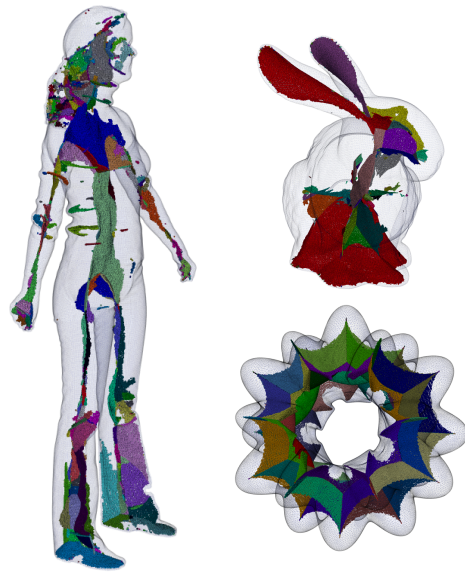


Figure 3: Points on the medial axis of three solids with triangle mesh boundaries computed with our method, described in [14]. The object angle threshold used is 0.6 radians.

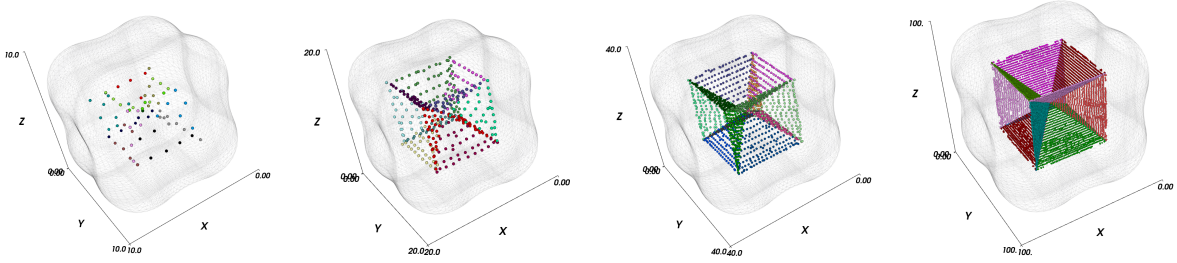


Figure 2: Medial points computed for the same solid with decreasing voxel size.

Ideally, if Algorithm 1 returns ‘Undetermined’ and a medial point m lies in S , m should not be a significant medial point, such as one of high object angle and radius. In [13], we described an algorithm based on an analysis of ∇D vectors in 2D and showed that the medial points missed by the algorithm become less significant as the density of samples on a circle increases. However, designing effective tools for detecting medial points in the 3D case is challenging. The next section describes a situation in which a significant medial point lies in S , while Algorithm 1 returns ‘Undetermined’.

3 Deep Samples

Suppose that $\text{DECIDEMA}(\mathcal{B}, S, \Phi)$ returns ‘Undetermined’. It may happen that none of the line segments $(\phi, \text{opp}(\phi))$ is long enough to penetrate deeply into S and none intersects the medial axis. As a result, it is possible to fail to detect medial points in S , as shown in Figure 4. The medial points missed in this example are of the highest object angle possible ($\pi/2$ for the medial point at the sphere centre). Further, as the radius of S can be chosen to be arbitrarily large, the medial points missed have arbitrarily large radius.

In order to improve the ability of Algorithm 1 to detect significant medial points, we propose to consider two additional query points c_{in} and c_{out} , defined as follows. Let the centre of S be c . Let the nearest point on the boundary \mathcal{B} to c be C , which is outside S by the assumption that S does not intersect \mathcal{B} . Define $c_{in}, c_{out} \in S$, where c_{out} is the intersection of S and the ray at c with direction $\overrightarrow{(c, C)}$ and c_{in} is the intersection of S and the ray at c with direction $\overrightarrow{(C, c)}$. Line

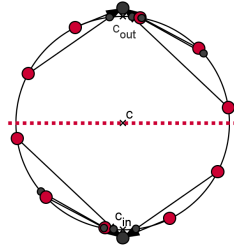


Figure 4: When \mathcal{B} consists of two points outside the sphere, the medial axis is shown as a dashed line. Points Φ are big dots on the sphere.

segment (c_{in}, c_{out}) is the longest line segment possible connecting a pair of points on S . In the example in Figure 4, $\nabla D(c_{in}) \neq \nabla D(c_{out})$. Therefore, in this example, by including c_{in} and c_{out} among the sampled points on S , we are guaranteed to detect a medial axis point in S . If we still do not detect a medial point in S , Lemma 2 characterizes where the set of nearest boundary points to points sampled on S must lie.

In the proof of the following lemma, we use $B(a, A)$ to denote a closed ball centred at point a and having point A on its boundary. Let $\Theta = \Phi \cup \{\text{opp}(\phi_i) | \phi_i \in \Phi\}$ be the set of all sampled points considered on S .

Lemma 2 *If $\nabla D(c_{in}) = \nabla D(c_{out})$ and $\text{DECIDEMA}(\mathcal{B}, S, \Phi)$ returns ‘Undetermined’, then all the nearest points on \mathcal{B} to points in Θ lie above the plane π through c_{in} with normal (c, C) .*

Proof. Consider point $p \in \Theta$ whose nearest boundary point is P . Consider the quantity $(P-p) \cdot N_S(p)$, where $N_S(p)$ is the outer normal to S at p . If $(P-p) \cdot N_S(p) > 0$, let p be $\text{opp}(p)$. Then $(P-p) \cdot N_S(p) \leq 0$.

The nearest point on \mathcal{B} to p , P , is inside or on the ball $B_p = B(p, C)$ and outside or on the ball $B_{c_{in}} = B(c_{in}, C)$. Refer to Figure 5. Consider the plane of intersection of $B_{c_{in}}$ and B_p , π_1 . Consider also the tangent plane to S at p , π_2 . Consider the plane ρ passing through the points p, c_{in}, c_{out} . Plane ρ is orthogonal to planes π, π_1 and π_2 .

Consider the orthogonal projection of P into ρ . Let (c_{in}, c_{out}) be vertical in ρ . Then P 's orthogonal projection lies in the half-plane left of $\pi_1 \cap \rho$ and in the half-plane bounded by $\pi_2 \cap \rho$ containing c . Let p' be the intersection of planes ρ, π_1 and π_2 . We will show that p' lies above π , and hence, P lies above π . Consider the line l through p and c_{in} . Note that $\angle c_{out}pc_{in} = \pi/2$ and $\angle Cpc_{in} > \pi/2$, since C is outside S . Let p'' be the intersection of the line l with π_1 . Since $\angle Cpc_{in} > \pi/2$ and l is orthogonal to π_1 , p'' is left of p on l . Hence, p'' , just like p , is above π . Since π_2 is tangent to S at p and since p'' is left of p on l , p' is above l on $\pi_2 \cap \rho$ and hence, above π . \square

Lemma 2 explains how using the sample points c_{in}

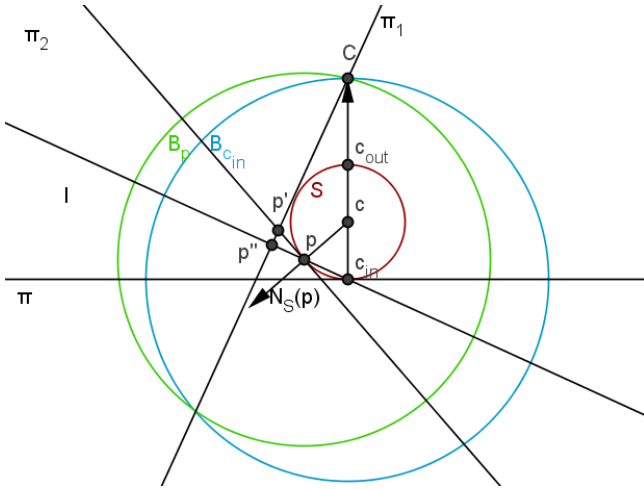


Figure 5: Side view at the objects of interest in the proof of Lemma 2.

and c_{out} restricts the situations where Algorithm 1 returns ‘Undetermined’. The next section explains how the set of all possible locations of the two nearest boundary points to a medial point missed by Algorithm 1 can be computed.

4 Nearest Boundary Points to Missed Medial Points

Suppose that Algorithm 1, $\text{DECIDEMA}(\mathcal{B}, S, \Phi)$, returns ‘Undetermined’. Consider the convex hull of the points $\Theta = \Phi \cup \{\text{opp}(\phi_i) \mid \phi_i \in \Phi\}$, $CH(\Theta)$. Suppose that there is a medial point m inside $CH(\Theta)$. We would like to know the locations of m ’s nearest points on \mathcal{B} .

Recall that $B_a = (a, A)$ is a closed ball with centre a having point A on its boundary and let $d(a, b)$ be the Euclidean distance between points a and b . The following tool will prove helpful in locating the nearest boundary points to m :

Lemma 3 Consider two closed balls $B_a = B(a, Y)$ and $B_b = B(b, Y)$. Then for any ball $B_c = B(c, Y)$, $c \in (a, b)$, $B_c \subseteq B_a \cup B_b$.

Proof.¹ Let x be the intersection of line segment (a, b) with $B_a \cap B_b$ (a disk). Let I be the boundary of $B_a \cap B_b$ (a circle). We want to show that the distance from c to I is less than or equal to $d(c, Y)$. Let $X \in I$. Then $d(c, X)^2 = d(c, x)^2 + d(x, X)^2$. Also $d(c, Y)^2 = d(c, x)^2 + d(x, Y)^2$. However, note that $d(x, X)^2 = d(x, Y)^2$, since X and Y both lie on the circle I with centre x . It follows that $d(c, Y)^2 = d(c, X)^2$ and $d(c, X) = d(c, Y)$. Thus, B_c is contained in the union of B_a and B_b . \square

Let \mathbb{B} be the set of closest points on \mathcal{B} to Θ . Let $N = |\Phi|$. We will assume that there are exactly N

distinct points in \mathbb{B} (this holds when the boundary \mathcal{B} is C^1). We now explain how to construct a region of \mathbb{R}^3 that contains all the possible nearest boundary points to a medial point m inside $CH(\Theta)$. This region will be found by subtracting the ‘empty foam’ from the ‘full foam’, which we define and explain how to compute in the following discussion.

Empty Foam For each point $p \in \Theta$, if $P \in \mathbb{B}$ is the nearest boundary point to p , then ball $B_p = (p, P)$ has an empty interior and the only point on its boundary is P . Let $\mathcal{F}_e = \bigcup B_p \setminus \mathbb{B}$ be the union of balls hereafter called the *empty foam*.

Full Foam Consider the Voronoi diagram of \mathbb{B} , $VD(\mathbb{B})$. Since m is a medial point, it is not one of the points in Θ . Suppose that m is in A ’s Voronoi region, $V(A)$, $A \in \mathbb{B}$. Then m ’s nearest point on \mathcal{B} is no further than $d(m, A)$, i.e. its nearest boundary point is on or inside the ball $B_m = (m, A)$. Using the information about A ’s Voronoi neighbours, we will find the region of space that contains B_m . This region of space will be a union of balls, which we call the *full foam of A* , \mathcal{F}_f^A . The set $\mathcal{F}_f = \{\bigcup \mathcal{F}_f^P \mid P \in \mathbb{B}\}$ is called the *full foam*.

We now explain how the full foam of A can be computed.

Let $\{a, \text{opp}(a)\} \subset \Theta$ be the points in Θ that have A as their nearest boundary point. Let a' be the nearest point on the line segment $(a, \text{opp}(a))$ to m . It can be easily shown that the nearest boundary point to a' is A . Consider the ray at a' with direction (a', m) . Let m' be the intersection of this ray with either the boundary of $V(A)$, or $CH(\Theta)$, whichever occurs first. Let $B_{m'} = B(m', A)$. Let $B_{a'} = B(a', A)$. By Lemma 3, $B_m \subset B_{a'} \cup B_{m'}$. Let $B_a = B(a, A)$ and $B_{\text{opp}(a)} = B(\text{opp}(a), A)$. By Lemma 3, $B_{a'} \subset B_a \cup B_{\text{opp}(a)}$. We add B_a and $B_{\text{opp}(a)}$ to \mathcal{F}_f^A and now proceed to find spheres that contain $B_{m'}$.

There are several cases: (1) m' is on a Voronoi face, (2) m' is on a Voronoi edge, (3) m' is on a Voronoi vertex, or (4) m' is on $CH(\Theta)$. We consider each case in turn.

Case 1. Suppose that the Voronoi face is a bisector of points A and B in \mathbb{B} . Let $\text{bis}(A, B)$ denote the bisector of points A and B . It is a plane. Consider a plane at m' with normal direction (a, A) . This plane necessarily intersects $\text{bis}(A, B)$ as (a', m) is necessarily not parallel to (a, A) and the intersection is a line on $\text{bis}(A, B)$ passing through m' . By following this line, we will find two points m_1^* and m_2^* , where each point either lies on an edge of $V(A)$ (Case 2), a vertex of $V(A)$ (Case 3), or on the $CH(\Theta)$ (Case 4). Define $B_{m_1^*} = B(m_1^*, A)$ and $B_{m_2^*} = B(m_2^*, A)$. Then $B_{m'} \subset B_{m_1^*} \cup B_{m_2^*}$ by Lemma 3. We now proceed to the respective cases to find balls containing $B_{m_1^*}$ and $B_{m_2^*}$.

Case 2. Suppose that the Voronoi edge of $V(A)$ is a trisector of points A , B and C in \mathbb{B} . Starting from a

¹We thank Nina Amenta for the idea behind this proof.

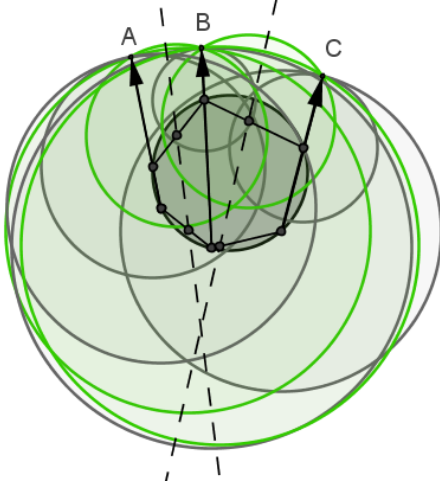


Figure 6: If a medial point m is in the convex hull of the 6 sampled points on the boundary of the dark disk with nearest boundary points A , B , and C , then the nearest boundary points to m are inside the green disk and outside the grey disks. The dashed lines are the bisectors of A , B and C .

point m^* on the edge, we will move up and down this edge until either we hit a Voronoi vertex of $V(A)$ (Case 3), or we hit the convex hull of Θ (Case 4) at points v_1 and v_2 . Then $m^* \in (v_1, v_2)$. Let $B_{v_1} = B(v_1, A)$ and $B_{v_2} = B(v_2, A)$. Then $B_{m^*} = B(m^*, A)$ is contained in $B_{v_1} \cup B_{v_2}$ by Lemma 3. We add B_{v_1} and B_{v_2} to the full foam of A \mathcal{F}_f^A .

Case 3. Any Voronoi vertex v of $V(A)$ inside $CH(\Theta)$ defines a ball $B_v = B(v, A)$ which we add to the full foam of A \mathcal{F}_f^A .

Case 4. In this case, $m' \in CH(\Theta)$. Suppose, for a contradiction, that m' is a vertex of $CH(\Theta)$. This vertex cannot be a or $\overrightarrow{opp(a)}$ because we reached it by following the direction (a', m) from a' . Any other point in Θ is outside of $V(A)$, and so is this vertex. But then we would have hit the boundary of $V(A)$ before hitting this vertex when following the ray $\overrightarrow{(a', m)}$ from a' . Therefore, m' lies on an edge of $CH(\Theta)$ (Case 5) or on the interior of some triangle of $CH(\Theta)$ (Case 6).

Case 5. In this case, point $m' \in V(A)$ lies on an edge e of $CH(\Theta)$. In case e is $(a, opp(a))$, then $B_{m'} = B(m', A)$ is contained in $B_a = B(a, A)$ and $B_{opp(a)} = B(opp(a), A)$ and these balls have already been added to \mathcal{F}_f^A . Suppose edge e is (a, b) or $(opp(a), b)$ for some point $b \in \Theta$ outside $V(A)$. Then $V(A)$ intersects (a, b) at some point x . By Lemma 3, either $B_{m'} \subset B_a \cup B_x$ or $B_{m'} \subset B_{opp(a)} \cup B_x$, where $B_x = B(x, A)$. In this case, we add B_x and either B_a or $B_{opp(a)}$ to \mathcal{F}_f^A . Now suppose edge e is (b, c) , which is intersected by $V(A)$, for some pair of points $b, c \in \Theta$ outside of $V(A)$. In

this case there are two points v_1 and v_2 on (b, c) that are the intersections of $V(A)$ with (b, c) , such that $m' \in (v_1, v_2)$. If $B_{v_1} = B(v_1, A)$ and $B_{v_2} = B(v_2, A)$, then $B_{m'} \subset B_{v_1} \cup B_{v_2}$. We add B_{v_1} and B_{v_2} to \mathcal{F}_f^A .

Case 6. In this case, point $m' \in V(A)$ lies on the interior of a triangle t of $CH(\Theta)$. At least one vertex of triangle t is a or $\overrightarrow{opp(a)}$. Suppose it is a . Then by following direction (a, m') , we will hit either (6-1) an edge of t at point m'' , or (6-2) the boundary of $V(A)$ at point m'' . Ball $B_{m'} = B(m', A)$ is contained in $B_a = B(a, A)$ and $B_{m''} = B(m'', A)$. In case 6-1, we proceed to Case 5 for point m'' (recalling that B_a is already in \mathcal{F}_f^A). In case 6-2, if m'' is on an edge or vertex of $V(A)$ and we add $B_{m''}$ to \mathcal{F}_f^A (recalling that B_a is already in \mathcal{F}_f^A). Otherwise, if m'' is on a face of $V(A)$, then the intersection of this face and t is a line segment (v_1, v_2) , where v_1 and v_2 are either on a Voronoi edge or vertex, or on an edge of t . If we define $B_{v_1} = B(v_1, A)$ and $B_{v_2} = B(v_2, A)$, then $B_{m'} \subset B_{v_1} \cup B_{v_2}$. In this case, we add B_{v_1} and B_{v_2} to \mathcal{F}_f^A (recalling that B_a is already in \mathcal{F}_f^A).

In this argument, for a medial point m in $CH(\Theta) \setminus V(A)$, we have added balls to \mathcal{F}_f^A passing through A centred at the following types of points q :

- **Type 1:** $q \in (a, opp(a))$
- **Type 2:** q is a vertex of $V(A)$ inside or on $CH(\Theta)$
- **Type 3:** q is an intersection of an edge of $V(A)$ with $CH(\Theta)$
- **Type 4:** q is an intersection of a face of $V(A)$ with edges of $CH(\Theta)$.

By the argument above, which uses multiple invocations of Lemma 3 to create a set of spheres that contain $B_m = B(m, A)$ for an arbitrarily positioned $m \in CH(\Theta) \setminus V(A)$, it follows that $B_m \subset \mathcal{F}_f^A$. Starting with an arbitrary point $m \in V(A)$, we can construct the full foam of A by taking the union of the four types of balls described above.

The union of the full foams of each boundary point $P \in \mathbb{B}$ gives the full foam: $\mathcal{F}_f = \{\bigcup \mathcal{F}_f^P \mid P \in \mathbb{B}\}$. Recall that the empty foam is $\mathcal{F}_e = \{\bigcup B_p \mid p \in \Theta \setminus \mathbb{B}\}$, where $B_p = B(p, P)$, and $P \in \mathbb{B}$ is the nearest boundary point to p . The region \mathcal{F}_e does not contain any points in \mathbb{B} .

We have shown the following lemma:

Lemma 4 *Suppose that $\text{DECIDEMA}(\mathbb{B}, S, \Theta)$ returned ‘Undetermined’. Let \mathbb{B} be the set of nearest boundary points to Φ and let $\Theta = \Phi \cup \{\overrightarrow{opp(\phi_i)} \mid \phi_i \in \Phi\}$. If there are exactly $|\Phi|$ distinct points in \mathbb{B} , then for any medial point $m \in CH(\Theta)$, its nearest boundary points lie in $\mathcal{F}_f \setminus \mathcal{F}_e$.*

Observe that when computing the full foam, we need only consider the vertices of $VD(\mathbb{B})$ inside or on $CH(\Theta)$,

the intersections of edges of $VD(\mathbb{B})$ with $CH(\Theta)$, and the intersection of faces of $VD(\mathbb{B})$ with edges of $CH(\Theta)$.

We can easily compute all the potential nearest boundary points to a medial point m in $CH(\Theta)$ by finding the intersection of the boundary \mathcal{B} with all the balls of the full foam of type 1-4. The quality of the approximation can be measured as the maximum distance between pairs of boundary points to missed medial points in $CH(\Theta)$, which is the maximum of the maximum distance between pairs of points in \mathcal{F}_f^A for all $A \in \mathbb{B}$.

5 Conclusions and Future Work

We have considered algorithms, based on the analysis of the gradient of the Euclidean distance transform on a sphere, that compute points within a user-chosen distance from the medial axis of an arbitrary 3D solid. Our experimental results on complex polyhedral inputs demonstrate that such an analysis of the ∇D vector field has a clear practical utility for the approximation of the medial axis. The contribution of this article has been to initiate the study of the quality of the approximation offered by such algorithms by establishing properties of the nearest boundary points to those medial points that are not detected. Much remains to be done in order to understand what theoretical guarantees can be offered by a method that studies a finite set of ∇D vectors in a fixed-radius spherical region in order to decide if this region is intersected by the medial axis in 3D and higher dimensions. Below we list several open problems. Medial point quality may be measured using either object angle, radius, or distance from the medial point to the query region.

1. Show that if $\text{DECIDEMA}(\mathcal{B}, S, \Phi)$ returns ‘Undetermined’, the quality of medial points present in sphere S decreases as the density of Φ increases.
2. Suppose that $\text{DECIDEMA}(\mathcal{B}, S, \Phi)$ returns ‘Undetermined’. For each sphere in \mathcal{F}_f , we add its centre to the set of query points Φ to create a set of query points Φ' . Next, execute $\text{DECIDEMA}(\mathcal{B}, S, \Phi')$. By carrying out this operation repeatedly, what can be said about the quality of the missed medial points as more iterations are considered?
3. Design other rules based on the analysis of a finite number of nearest boundary points to query points on a sphere that enable detection of medial points inside the sphere, such that the quality of the missed medial points can be shown to decrease by increasing the density of query points used, for a fixed-size query region S .

References

- [1] N. Amenta, S. Choi, and R. Kolluri. The power crust, unions of balls, and the medial axis transform. *Computational Geometry: Theory and Applications*, 19(2-3):127–153, 2001.
- [2] D. Attali and J.-O. Lachaud. Delaunay conforming iso-surface, skeleton extraction and noise removal. *Computational Geometry Theory and Applications*, 19(2-3):175–189, 2001.
- [3] H. Blum. Biological shape and visual science. *Journal of Theoretical Biology*, 38:205–287, 1973.
- [4] I. Boada, N. Coll, N. Madern, and J. A. Sellarès. Approximations of 2D and 3D generalized Voronoi diagrams. *Computer Mathematics*, 85(7):1003–1022, 2008.
- [5] T. Culver, J. Keyser, and D. Manocha. Exact computation of the medial axis of a polyhedron. *Computer Aided Geometric Design*, 21(1):65–98, 2004.
- [6] T. K. Dey and W. Zhao. Approximating the medial axis from the Voronoi diagram with a convergence guarantee. *Algorithmica*, 38:387–398, 2004.
- [7] M. Etzion and A. Rappoport. Computing Voronoi skeletons of a 3-d polyhedron by space subdivision. *Computational Geometry: Theory and Applications*, 21:87–120, 2002.
- [8] M. Foskey, M. C. Lin, and D. Manocha. Efficient computation of a simplified medial axis. In *Solid Modeling and Applications*, pages 96–107, 2003.
- [9] B. Miklos, J. Giesen, and M. Pauly. Discrete scale axis representations for 3D geometry. In *SIGGRAPH*, 2010.
- [10] K. Siddiqi, S. Bouix, A. R. Tannenbaum, and S. W. Zucker. Hamilton-Jacobi skeletons. *IJCV*, 48(3):215–231, 2002.
- [11] K. Siddiqi and S. Pizer, editors. *Medial representations: mathematics, algorithms and applications*. Springer, 2008.
- [12] S. Stolpner and K. Siddiqi. Revealing significant medial structure in polyhedral meshes. In *3DPVT*, pages 365–372, 2006.
- [13] S. Stolpner and S. Whitesides. Medial axis approximation with bounded error. In *International Symposium on Voronoi Diagrams*, pages 171–180, 2009.
- [14] S. Stolpner, S. Whitesides, and K. Siddiqi. Sampled medial loci for 3D shape representation. *CVIU*, 115:695–706, 2011.
- [15] R. Tam and W. Heidrich. Shape simplification based on the medial axis transform. In *Visualization*, page 63, 2003.
- [16] J. M. Vleugels and M. H. Overmars. Approximating generalized Voronoi diagrams in any dimension. Technical Report UU-CS-1995-14, Utrecht University, 1995.
- [17] Y. Yang, O. Brock, and R. N. Moll. Efficient and robust computation of an approximated medial axis. In *Solid Modeling and Applications*, pages 15–24, 2004.